RESONANCE FLUORESCENCE OF A DRIVEN TWO-LEVEL ATOM IN A CAVITY WITH INJECTED SQUEEZED VACUUM: EFFECT OF THE CAVITY FREQUENCY DETUNING. [1]

Peng Zhou[2], S. Swain[3]
Department of Applied Mathematics and Theoretical Physics,
The Queen's University of Belfast,
Belfast BT7 1NN, Northern Ireland, the United Kingdom.

We derive, in the bad cavity limit, an effective master equation for the reduced density matrix operator of a strongly driven atom coupled to a frequency-tunable cavity and damped by a squeezed vacuum. We find that the intensity, the resonance fluorescence spectrum and the photon-photon correlation of such an atom, emitted from the cavity, are strongly dependent upon the cavity resonance frequency and squeezing parameters. The enhancement and suppression of the fluorescence intensity and spectral peaks, spectral-line narrowing, and antibunching in fluorescence can be achieved in a prescribed manner by tuning the cavity and laser frequency, and by adjusting the squeezed photon number and phase.

1. Introduction

It is well-known that the radiative properties of atoms placed inside a cavity differ qualitatively from those in free space because of the modification of the surrounding electromagnetic modes, which are concentrated around the cavity resonant frequency [1]. For an excited atom located inside such a cavity, the cavity mode is the only one available to the atom for emission. The spontaneous emission rate into the particular cavity mode can be enhanced or inhibited [2] by tuning the cavity into or out-of resonance with the radiative atom. Cavity-enhanced and cavity-inhibited spontaneous emission, resulting in a broadening or narrowing of the spectrum, has been observed by several groups [3].

For a two-level atom placed inside a cavity and strongly driven by a coherent field, theoretical studies have predicted a phenomenological richness not found in the absence

---

of the coherent driving—for example, dynamical suppression of the spontaneous emission rate [4, 5], population inversion in both bare and dressed state bases [5, 6], distortion and narrowing [4, 5, 6] of the Mollow triplet and multipeaked spectral profiles [6, 7]. All these features are very sensitive to the cavity resonant frequency. Recently, Lange and Walther [8] have observed the dynamical suppression of spontaneous emission in a microwave cavity. In the optical-frequency regimes, Zhu *et al.* [9] have also reported experimental studies of the effects of the cavity detuning on the radiative properties of a coherently driven two-level atom. They have shown that the atomic fluorescence of a strongly driven two-level atom is enhanced when the cavity frequency is tuned to one of the sidebands of the Mollow fluorescence triplet, whereas it is inhibited by tuning to the other sideband. The enhancement of atomic fluorescence at one sideband is a direct demonstration of population inversion.

As many authors have stated [10–15], the cavity is the best candidate, from the experimental point of view, to investigate the interaction of atoms with nonclassical light. Since the atom interacts strongly only with the privileged cavity mode, only the modes within a small solid angle about this cavity mode need be squeezed, unlike in free space, where the squeezed modes must occupy the whole 4π solid angle of space. An exception is the linear dependence of the two-photon excitation probability for a three level ladder atom excited by the squeezed vacuum. This provided the first experimental study of atom/squeezed-light interactions, and was carried out in a confined magnetic-optical trap [16], which may be well modelled as a bad cavity [17].

For a cavity with a fixed resonance-frequency, Rice *et al.* [12] considered a weakly driven two-level atom ($\Omega \ll \kappa$) interacting with a squeezed vacuum injected via the input-output mirror of the cavity in the bad cavity limit, and found that the evolution of the atom is formally same as the one in free space, but with a renormalized decay constant ($\gamma + \gamma_c$). All the squeezing-induced effects predicted in free space, such as the phase-sensitive Mollow triplet [11], anomalous spectral features — hole-burning and dispersive profiles at line centre [18] and gain without population inversion [19], can thus be carried over to the cavity configuration [12]. For a strongly driven ($\Omega \geq \kappa$) two-level atom coupled to such a cavity, Cirac [13], predicted a squeezing-enhanced population inversion and a phase-sensitive Mollow spectrum with intensity-dependent linewidths. In the current paper we extend these studies to a strongly driven atom coupled to a *frequency-tunable* cavity mode damped by a squeezed vacuum. We shall see that a variety of novel features will be displayed by appropriately tuning the cavity frequency.

This paper is organized as follows: In Sec. 2 we derive, in the bad cavity limit, an effective master equation of the reduced density matrix operator for the strongly driven atom placed inside a frequency-tunable cavity which is damped by a broadband squeezed vacuum. It exhibits resonance properties when the cavity frequency is tuned to the centre and sidebands of the standard Mollow triplet. In Sec. 3 we report the modification of the resonance fluorescence of the atom emitted from the side of the cavity, in terms of the intensity spectrum and intensity-intensity correlation, which are found to depend strongly on the cavity resonance frequency. The final section contains a summary.

2. The model

We consider a single two-level atom with transition frequency ω_A coupled to a single-mode cavity field of frequency ω_C. The atom is driven by a coherent laser of frequency ω_L. The cavity is damped, via the input-output mirror, by a broadband squeezed vacuum with carrier frequency ω_s which is locked to the laser frequency ω_L for simplicity. The cavity mode is described by annihilation and creation operators a and $a^\dagger$, while the atom is represented by the usual Pauli spin-$\frac{1}{2}$ operators σ_+, σ_-, which satisfy the commutation relations $[\sigma_+, \sigma_-] = \sigma_z$ and $[\sigma_z, \sigma_\pm] = \pm 2\sigma_\pm$. In a frame rotating at the frequency ω_L the master equation of the density matrix operator ρ for the combined atom-cavity system is [12, 13, 14, 15]

$$\dot{\rho} = -i\left[H_A + H_C + H_I,\, \rho\right] + \mathcal{L}_A \rho + \mathcal{L}_C \rho, \tag{1}$$

where

$$
\begin{aligned}
H_A &= \frac{\Delta}{2}\sigma_z + \frac{\Omega}{2}(\sigma_+ + \sigma_-), & (2)\\
H_C &= \delta\, a^\dagger a, & (3)\\
H_I &= ig\left(\sigma_- a^\dagger - \sigma_+ a\right), & (4)\\
\mathcal{L}_A \rho &= \gamma(2\sigma_- \rho\sigma_+ - \sigma_+\sigma_-\rho - \rho\sigma_+\sigma_-), & (5)\\
\mathcal{L}_C \rho &= \kappa(N+1)\left(2a\rho a^\dagger - a^\dagger a\rho - \rho a^\dagger a\right) + \kappa N\left(2a^\dagger\rho a - aa^\dagger\rho - \rho aa^\dagger\right) \\
&\quad - \kappa M\left[e^{i\Phi}\left(2a^\dagger\rho a^\dagger - a^{\dagger 2}\rho - \rho a^{\dagger 2}\right) + h.c.\right], & (6)
\end{aligned}
$$

H_A and H_C are the unperturbed Hamiltonians for the coherently driven atom and the cavity respectively, while H_I describes the interaction between the atom and the cavity mode. Ω is the Rabi frequency of the driving field, $\Delta = \omega_A - \omega_L$ and $\delta = \omega_C - \omega_L$ are the detunings of the atomic resonance frequency and of the cavity-mode frequency from the driving field frequency respectively, g is the coupling constant between the atom and the cavity field, and $\Phi = \phi_s - 2\phi_L$ is the relative phase between the squeezed vacuum (ϕ_s) and the laser field (ϕ_L). (Note that we have re-defined the operators $\sigma_+ = \sigma_+ \exp(i\phi_L)$ and $a = a\exp(-i\phi_L)$ in the above equations, in order to merge the phases .) $\mathcal{L}_A \rho$ and $\mathcal{L}_C \rho$ respectively describe atomic damping to background modes other than the privileged cavity mode, and damping of the cavity field by a broadband squeezed vacuum reservoir, with γ and κ the atomic and cavity decay constants respectively.

The real parameters N and M are the photon number and the strength of the two-photon correlations in the broadband squeezed vacuum. They obey the relation $M = \eta\sqrt{N(N+1)}$, where the quantity $0 \leq \eta \leq 1$ measures the degree of two photon correlations in the squeezed vacuum. We take $\eta = 1$ throughout, that is, the squeezed vacuum is injected into the cavity with the maximum two-photon correlation.

In this paper we are interested in the bad cavity limit, *i.e.*, the cavity has a low Q value, and the atom-cavity coupling is weak, so that $\kappa \gg g \gg \gamma$, and the cavity field decay dominates. The cavity field response to the continuum modes is much faster than that produced by its interaction with the atom, so that the atom always experiences the cavity mode in the state induced by the vacuum reservoir. Thus one can adiabatically

eliminate the cavity-mode variables, giving rise to a master equation for the atomic variables only. As the procedure for eliminating the cavity mode in this paper is similar to the one in Refs.[5, 8, 13], we refer readers to these references for the details, and here only outline the key points.

We temporarily disregard $\mathcal{L}_A \rho$ in the elimination of the cavity-mode, since it unchanged by the following operations. First we perform canonical transformations on the master equation (1):

$$\tilde{\rho} = SU(t)\rho U^\dagger(t)S^\dagger, \tag{7}$$

where $U(t) = \exp\left[i\left(H_A + H_C\right)t\right]$, and S is the usual squeeze operator that transforms the annihilation operator as $SaS^\dagger = \mu a + \nu a^\dagger$. The right-hand side (r.h.s.) of (7) represents a sequential transform of the density operator ρ to the atom-cavity interaction picture and the squeezed picture. If we take $\mu = \sqrt{N+1}$ and $\nu = \sqrt{N}\exp[i\left(\Phi + 2\delta\right)t]$, the master equation (1) is then transformed to

$$\dot{\tilde{\rho}} = -i[\tilde{H}_I(t), \tilde{\rho}] + \mathcal{L}_{vac}\tilde{\rho}, \tag{8}$$

where

$$\mathcal{L}_{vac}\tilde{\rho} = \kappa\left(2a\tilde{\rho}a^\dagger - a^\dagger a\tilde{\rho} - \tilde{\rho}a^\dagger a\right), \tag{9}$$

$$\tilde{H}_I(t) = g\left[\tilde{D}_+(t)ae^{-i\delta t} + h.c.\right], \tag{10}$$

with

$$\tilde{D}_+(t) = i\left[\sqrt{N}e^{-i\Phi}\tilde{\sigma}_-(t) - \sqrt{N+1}\tilde{\sigma}_+(t)\right],$$

$$\tilde{\sigma}_\pm(t) = e^{iH_A t}\sigma_\pm e^{-iH_A t}. \tag{11}$$

$\tilde{H}_I(t)$ now indicates the effective atom-cavity coupling, whilst $\mathcal{L}_{vac}\tilde{\rho}$ describes the cavity loss due to its coupling to an electromagnetic reservoir in a vacuum state. That is the transformed cavity mode is damped by a standard vacuum, and the effect of the squeezed reservoir is transferred to the effective atom-cavity interaction.

We next introduce the operator χ [5, 8, 13, 20]

$$\chi = e^{-\mathcal{L}_{vac}t}\tilde{\rho}, \tag{12}$$

which, according to Eq. (8), obeys the equation

$$\dot{\chi}(t) = -ige^{\kappa t}\{[a^\dagger, \tilde{D}_-(t)\chi(t)]e^{i\delta t} + [a, \chi(t)\tilde{D}_+(t)]e^{-i\delta t}\}$$
$$-ige^{-\kappa t}\{[\tilde{D}_-(t), \chi(t)a^\dagger]e^{i\delta t} + [\tilde{D}_+(t), a\chi(t)]e^{-i\delta t}\}. \tag{13}$$

Only the atom-cavity interaction is involved. Due to the smallness of the coupling constant g, we can perform a second-order perturbation calculation with respect to g by means of standard projection operator techniques. Noting that $\mathrm{Tr}_C\chi(t) \equiv \mathrm{Tr}_C\tilde{\rho}(t) \equiv \tilde{\rho}_A(t)$, we can trace out the cavity variables to obtain the master equation for the reduced

density matrix operator $\tilde{\rho}_A$ of the atom. Under the Born-Markovian approximation, the resulting master equation is

$$\tilde{\rho}_A(t) = -g^2 \int_0^\infty \left\{ e^{-(\kappa - i\delta)\tau} [\tilde{\rho}_A(t)\tilde{D}_+(t - \tau)\tilde{D}_-(t) - \tilde{D}_-(t)\tilde{\rho}_A(t)\tilde{D}_+(t - \tau)] + h.c. \right\} d\tau. \tag{14}$$

Finally transforming $\tilde{\rho}_A$ back to the original picture via $\rho_A = \exp(-iH_A t)\tilde{\rho}_A \exp(iH_A t)$ and Eq. (11), and restoring the $\mathcal{L}_A \rho_A$ contribution, one finds the atomic master equation to be

$$\begin{aligned}
\dot{\rho}_A &= -i\,[H_A,\,\rho_A] \\
&\quad + \gamma_c(N+1)\,(\sigma_-\rho_A A_+ - \rho_A A_+\sigma_- + B_-\rho_A\sigma_+ - \sigma_+ B_-\rho_A) \\
&\quad + \gamma_c N\,(\sigma_+\rho_A A_- - \rho_A A_-\sigma_+ + B_+\rho_A\sigma_- - \sigma_- B_+\rho_A) \\
&\quad - \gamma_c M e^{i\Phi}\,(\sigma_+\rho_A A_+ - \rho_A A_+\sigma_+ + B_+\rho_A\sigma_+ - \sigma_+ B_+\rho_A) \\
&\quad - \gamma_c M e^{-i\Phi}\,(\sigma_-\rho_A A_- - \rho_A A_-\sigma_- + B_-\rho_A\sigma_- - \sigma_- B_-\rho_A) \\
&\quad + \gamma\,(2\sigma_-\rho_A\sigma_+ - \sigma_+\sigma_-\rho_A - \rho_A\sigma_+\sigma_-).
\end{aligned} \tag{15}$$

The first term on the r.h.s. of the master equation describes the coherent evolution of the driven atom, whereas the following four terms represent the cavity-induced atomic decay into the cavity-mode with the rate $\gamma_c = g^2/\kappa$. The last term shows the atomic decay into the background modes with the rate γ. The other parameters in Eq. (15) are defined as

$$\begin{aligned}
A_+ &= (B_-)^\dagger = \kappa \int_0^\infty d\tau\, e^{-(\kappa - i\delta)\tau}\tilde{\sigma}_+(-\tau) = \alpha_0\sigma_z + \alpha_1\sigma_- + \alpha_2\sigma_+, \\
A_- &= (B_+)^\dagger = \kappa \int_0^\infty d\tau\, e^{-(\kappa - i\delta)\tau}\tilde{\sigma}_-(-\tau) = \beta_0\sigma_z + \beta_1\sigma_+ + \beta_2\sigma_-
\end{aligned} \tag{16}$$

with

$$\begin{aligned}
\alpha_0 &= \frac{\kappa\Omega}{4\bar{\Omega}^2}\left[\frac{2\Delta}{\kappa - i\delta} - \frac{\bar{\Omega} + \Delta}{\kappa - i(\delta - \bar{\Omega})} + \frac{\bar{\Omega} - \Delta}{\kappa - i(\delta + \bar{\Omega})}\right], \\
\beta_0 &= \frac{\kappa\Omega}{4\bar{\Omega}^2}\left[\frac{2\Delta}{\kappa - i\delta} - \frac{\bar{\Omega} + \Delta}{\kappa - i(\delta + \bar{\Omega})} + \frac{\bar{\Omega} - \Delta}{\kappa - i(\delta - \bar{\Omega})}\right], \\
\alpha_1 = \beta_1 &= \frac{\kappa\Omega^2}{4\bar{\Omega}^2}\left[\frac{2}{\kappa - i\delta} - \frac{1}{\kappa - i(\delta - \bar{\Omega})} - \frac{1}{\kappa - i(\delta + \bar{\Omega})}\right], \\
\alpha_2 &= \frac{\kappa}{4\bar{\Omega}^2}\left[\frac{2\Omega^2}{\kappa - i\delta} + \frac{(\bar{\Omega} + \Delta)^2}{\kappa - i(\delta - \bar{\Omega})} + \frac{(\bar{\Omega} - \Delta)^2}{\kappa - i(\delta + \bar{\Omega})}\right], \\
\beta_2 &= \frac{\kappa}{4\bar{\Omega}^2}\left[\frac{2\Omega^2}{\kappa - i\delta} + \frac{(\bar{\Omega} + \Delta)^2}{\kappa - i(\delta + \bar{\Omega})} + \frac{(\bar{\Omega} - \Delta)^2}{\kappa - i(\delta - \bar{\Omega})}\right],
\end{aligned} \tag{17}$$

where $\bar{\Omega} = \sqrt{\Omega^2 + \Delta^2}$ is a generalized Rabi frequency. Obviously, the coefficients $\mathcal{A}_0$, $\mathcal{A}_1$, $\mathcal{A}_2$ are Rabi-frequency-dependent, and resonant when the cavity frequency is tuned to $\delta = 0, \pm\bar{\Omega}$, which is reminiscent of the Mollow triplet in free space [21]. The

resonance property reflects the fact that when the atom is strongly driven by a laser beam, the atom-laser interaction forms a 'dressed' atom [22] whose energy-level structure is intensity-dependent and whose spontaneous emission dominates at the three frequencies ω_L, and $\omega_L \pm \bar{\Omega}$. Therefore, when the cavity is tuned to these three frequencies, atomic transitions are enhanced.

From the master equation (15), one obtains the optical Bloch equations, in terms of the in-phase and out-of-phase quadrature amplitudes of the atomic polarization, $\langle \sigma_x \rangle = \langle \sigma_- \rangle + \langle \sigma_+ \rangle$ and $\langle \sigma_y \rangle = i(\langle \sigma_- \rangle - \langle \sigma_+ \rangle)$, and the atomic population difference $\langle \sigma_z \rangle$, to be

$$\langle \dot{\sigma}_x \rangle = -\gamma_x \langle \sigma_x \rangle - \Delta_y \langle \sigma_y \rangle + \Omega_1,$$
$$\langle \dot{\sigma}_y \rangle = -\gamma_y \langle \sigma_y \rangle + \Delta_x \langle \sigma_x \rangle - \Omega \langle \sigma_z \rangle - \Omega_2,$$
$$\langle \dot{\sigma}_z \rangle = -\gamma_z \langle \sigma_z \rangle + \Omega_x \langle \sigma_x \rangle + \Omega_y \langle \sigma_y \rangle - \Gamma_0, \tag{18}$$

where

$$
\begin{aligned}
\gamma_x &= \gamma - \gamma_c \operatorname{Re}\left[(\alpha_1 - \alpha_2)\left(N + 1 + Me^{i\Phi}\right) + (\beta_1 - \beta_2)\left(N + Me^{-i\Phi}\right)\right], \\
\gamma_y &= \gamma + \gamma_c \operatorname{Re}\left[(\alpha_1 + \alpha_2)\left(N + 1 - Me^{i\Phi}\right) + (\beta_1 + \beta_2)\left(N - Me^{-i\Phi}\right)\right], \\
\gamma_z &= \gamma_x + \gamma_y, \\
\Delta_x &= \Delta + \gamma_c \operatorname{Im}\left[(\alpha_1 - \alpha_2)\left(N + 1 - Me^{i\Phi}\right) - (\beta_1 - \beta_2)\left(N - Me^{-i\Phi}\right)\right], \\
\Delta_y &= \Delta - \gamma_c \operatorname{Im}\left[(\alpha_1 + \alpha_2)\left(N + 1 + Me^{i\Phi}\right) - (\beta_1 + \beta_2)\left(N + Me^{-i\Phi}\right)\right], \\
\Omega_x &= 2\gamma_c \operatorname{Re}\left[\alpha_0\left(N + 1 - Me^{i\Phi}\right) + \beta_0\left(N - Me^{-i\Phi}\right)\right], \\
\Omega_y &= \Omega + 2\gamma_c \operatorname{Im}\left[\alpha_0\left(N + 1 + Me^{i\Phi}\right) - \beta_0\left(N + Me^{-i\Phi}\right)\right], \\
\Omega_1 &= 2\gamma_c \operatorname{Re}\left[\alpha_0\left(N + 1 + Me^{i\Phi}\right) - \beta_0\left(N + Me^{-i\Phi}\right)\right], \\
\Omega_2 &= -2\gamma_c \operatorname{Im}\left[\alpha_0\left(N + 1 - Me^{i\Phi}\right) + \beta_0\left(N - Me^{-i\Phi}\right)\right], \\
\Gamma_0 &= 2\gamma + 2\gamma_c \operatorname{Re}\left[\alpha_2(N + 1) - \beta_2 N + \alpha_1 Me^{i\Phi} - \beta_1 Me^{-i\Phi}\right], \tag{19}
\end{aligned}
$$

and γ_x, γ_y and γ_z are the relaxation rates of the phase quadratures of the atomic polarization and of the population difference respectively. As in the case of free space [10], the relaxation rates of the polarization quadratures are unequal and phase-sensitive. On the other hand, the rates are also resonant at different cavity frequencies. For example, for $\Delta = 0$, the rates become

$$
\begin{aligned}
\gamma_x &= \gamma + \frac{\gamma_c}{2}\left[\frac{\kappa^2}{\kappa^2 + (\delta - \Omega)^2} + \frac{\kappa^2}{\kappa^2 + (\delta + \Omega)^2}\right](2N + 1 + 2M\cos\Phi), \\
\gamma_y &= \gamma + \gamma_c \frac{\kappa^2}{\kappa^2 + \delta^2}(2N + 1 - 2M\cos\Phi). \tag{20}
\end{aligned}
$$

The first is resonant with the cavity frequency tuned to the Rabi sidebands, $\delta = \pm\Omega$, whilst the resonance in γ_y takes place at the cavity frequency $\delta = \omega_C - \omega_L = 0$. With increasing Rabi frequency, the decay rate γ_x of the in-phase dipole quadrature can be significantly suppressed at the cavity frequency $\delta = 0$.

It is not different to show that the Bloch equations (18) reduce to Cirac's case, *i.e.* Eqs. (3.2) and (3.3) in Ref. [13], when the cavity and driving frequencies are same: $\delta = 0$. When the atom, driving laser and cavity mode are all in resonance ($\Delta = \delta = 0$) and the Rabi frequency is much less than the cavity linewidth ($\Omega \ll \kappa$), the equations (18) become the ones obtained by Rice *et al.* [12], which are formally similar to those in free space, but with the renormalized decay rate $\gamma + \gamma_c$. In the present paper we shall mainly focus on the effect of the cavity frequency on the resonance fluorescence of a strongly driven two-level atom ($\Omega \geq \kappa$). As we shall see, the fluorescent emission from such an atom can be dramatically modified by tuning the frequency of the cavity to the centre or sidebands of the Mollow triplet.

3. Resonance fluorescence

3.1. The Intensity

One of the observables of interest is the steady-state fluorescence intensity of the atom emitted from the side of the cavity, which is proportional to the steady-state population in the excited state:

$$I_s \propto \langle \sigma_{11} \rangle_s = \frac{\Omega_1 \left(\Omega_x \gamma_y + \Delta_x \Omega_y \right) + \left(\Omega_2 - \Omega \right) \left(\Omega_x \Delta_y - \gamma_x \Omega_y \right) + \left(\gamma_z - \Gamma_0 \right) \left(\gamma_x \gamma_y + \Delta_x \Delta_y \right)}{2 \left[\left(\gamma_x \gamma_y + \Delta_x \Delta_y \right) \gamma_z + \Omega \left(\gamma_x \Omega_y - \Omega_x \Delta_y \right) \right]}. \tag{21}$$

We plot the intensity against the cavity frequency (detuning) in Figs. 1 and 2, where the former corresponds to the situation where the driving laser is resonant with the atom ($\Delta = 0$), while the latter is for the laser detuned from the atom ($\Delta = 100$). The solid, dashed and dot-dashed curves in these two figures are for $\Phi = 0$, $\pi/2$ and π respectively, whereas the other parameters are (a) $\Omega = 100$, $N = 0.5$; (b) $\Omega = 100$, $N = 2$; (c) $\Omega = 500$, $N = 0.5$ and (d) $\Omega = 500$, $N = 2$. In this paper we work in the bad cavity limit, so we set $\kappa = 100$, $g = 30$, $\gamma = 1$ throughout the following graphics. (Note that all parameters are scaled in the unit of $\gamma = 1$.)

These figures show clearly that the atomic fluorescence intensity emitted out the cavity walls varies dramatically with the cavity and driving laser frequencies, the laser intensity and the squeezing phase (the effect of the two-photon correlations [15]). When the laser field is resonant with the atom, shown in Fig. 1, the intensity for the squeezing phase $\Phi = 0$ is resonantly enhanced at the cavity frequency tuned to the frequency of the driving laser, *i.e.*, $\delta = 0$. However, for the squeezing phase $\Phi = \pi$, the intensity is suppressed at $\delta = 0$, while it may be resonantly enhanced at the cavity frequency tuned close to the Rabi sideband, $\delta \sim \pm\Omega$. The resonance profile at the central frequency is a Lorentzian lineshape, whereas it is a Rayleigh-wing lineshape at the Rabi sidebands. For certain laser intensities and squeezing photon numbers, the resonance profile at the sidebands may so very weak as to be invisible − see for instance, Fig. 1b. For other squeezing phases, say $\Phi = \pi/2$, the intensity is asymmetric around the cavity detuning $\delta = 0$. Specifically, the fluorescence emission of the atom out of the cavity is enhanced for $\delta > 0$, and suppressed for $\delta < 0$.
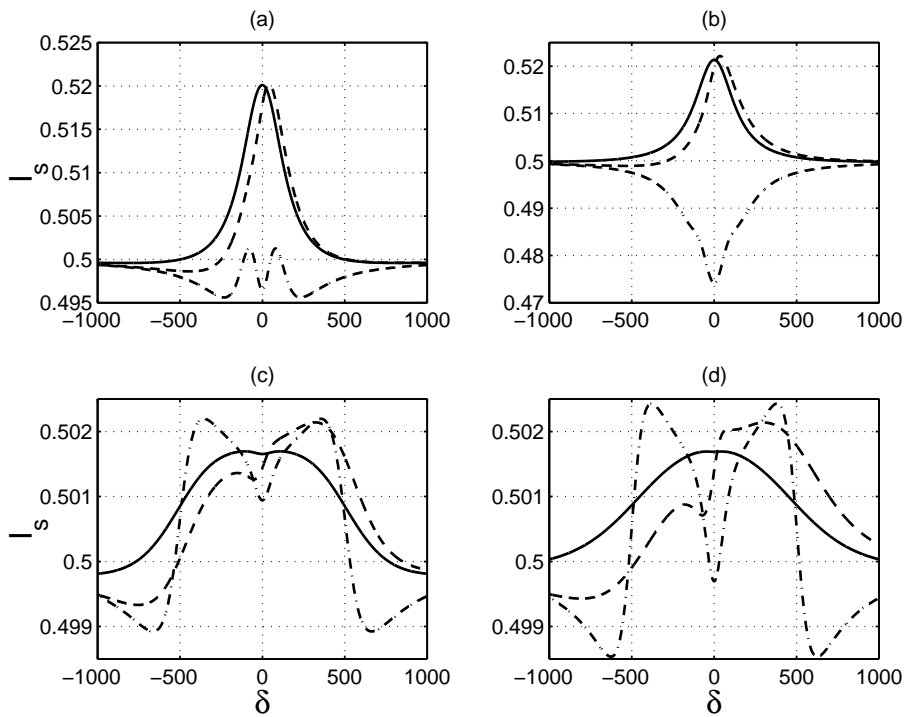
Fig. 1. The steady-state fluorescence intensity I_s as a function of the cavity detuning δ, for the parameters: $\kappa = 100$, $g = 30$, $\gamma = 1$, $\Delta = 0$, and (a): $\Omega = 100$, $N = 0.5$, (b): $\Omega = 100$, $N = 2$, (c): $\Omega = 500$, $N = 0.5$, (d): $\Omega = 500$, $N = 2$. In these frames the solid, dashed and dot-dashed curves are respectively for $\Phi = 0$, $\pi/2$ and π. (All parameters are set in the unit of $\gamma = 1$ throughout the graphs in this paper.)

When the laser field is detuned from the atomic transition frequency, the fluorescence intensity, depicted in Fig. 2 for $\Delta = 100$, is asymmetric about $\delta = 0$ for all squeezing phases. The intensity is remarkably enhanced when the cavity frequency is tuned to the lower-frequency Rabi sideband, $\delta = -\bar{\Omega}$, while it is suppressed at the other sideband, $\delta = \bar{\Omega}$. Note that the resonance profiles are opposite to those in Fig. 1, that is, a Lorentzian lineshape when the cavity frequency is tuned to the Rabi sidebands, and a Rayleigh-wing shape when the cavity frequency is tuned to the central of the Mollow triplet.

The enhancement of the fluorescence intensity is a direct consequence of the population inversion ($\langle \sigma_{11} \rangle_s > 0.5$), which results from the coupling of the atom to the cavity mode [5, 9, 23]. Cirac's study [13] of a driven two-level atom coupled to a fixed-frequency cavity mode tuned to the laser frequency predicted that squeezed vacuum damping of the cavity mode enhances the cavity-induced inversion by a tiny amount. However, we find that the population inversion may be significantly enhanced if the cavity frequency is tuned to one of the Rabi sidebands. For example in Fig. 2b, a large inversion $(\langle \sigma_{11} \rangle_s - \langle \sigma_{00} \rangle_s) \sim 0.25$ is achieved at the cavity detuning $\delta \sim -\bar{\Omega}$.

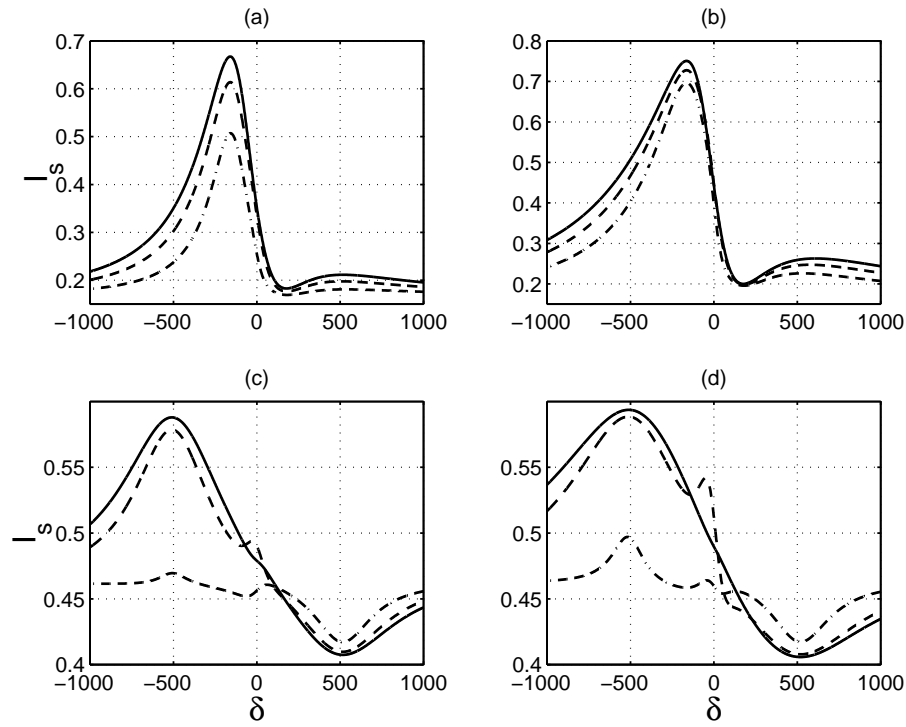On the other hand, Cabrillo and Swain [15] have recently proposed detecting the

Fig. 2. Same as Fig. 1, but with $\Delta = 100$.

quantum two-photon correlation in a squeezed vacuum via measuring the phase-sensitive internal cavity photon number. Our results show that the fluorescence intensity of the atom emitted from the side of the cavity is also phase-dependent. Alternatively, one may measure the quantum correlation by recording the atomic fluorescence photons emitted out of the cavity.

3.2. The Spectrum

The incoherent fluorescence spectrum of the atom, emitted from the side of the cavity, can be calculated in term of the two-time correlation function $\lim_{t\to\infty} \langle \sigma_+ (t+\tau), \sigma_- (t) \rangle$ by invoking the quantum regression theorem together with the optical Bloch equations (18). The spectrum is of the form,

$$\Lambda(\omega) = \tfrac{1}{2}\,\mathrm{Re} \left\{ \frac{\left[(\gamma_y + z + i\Delta_x)\,(\gamma_z + z) + \Omega\,(\Omega_y - i\Omega_x)\right] \chi_1}{\left[(\gamma_x + z)\,(\gamma_y + z) + \Delta_x\Delta_y\right](\gamma_z + z) + \Omega\left[(\gamma_x + z)\,\Omega_y - \Omega_x\Delta_y\right]} \right. \tag{22}$$
$$\left. - \frac{\left[\Delta_y - i\,(\gamma_x + z)\right]\left[(\gamma_z + z)\,\chi_2 - \Omega\chi_3\right]}{\left[(\gamma_x + z)\,(\gamma_y + z) + \Delta_x\Delta_y\right](\gamma_z + z) + \Omega\left[(\gamma_x + z)\,\Omega_y - \Omega_x\Delta_y\right]} \right\}_{z=i\omega}$$

with

$$\chi_1 = \frac{1}{2}\left(1 + \langle\sigma_z\rangle_s - \langle\sigma_x\rangle_s^2 + i\langle\sigma_x\rangle_s\langle\sigma_y\rangle_s\right),$$
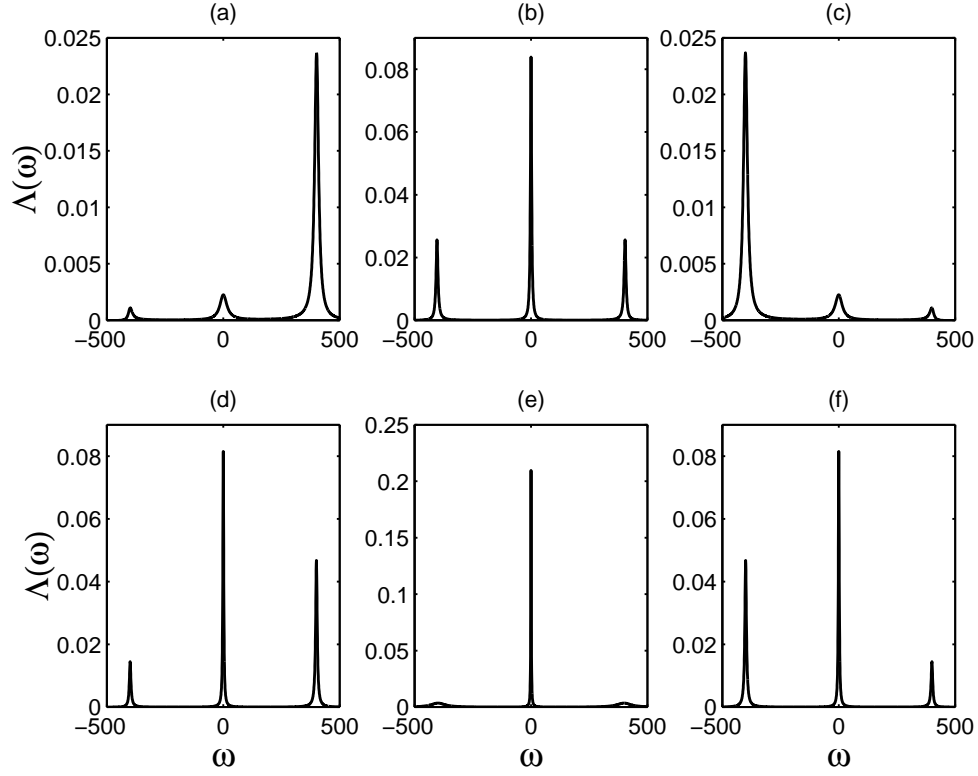
Fig. 3. The incoherent resonance fluorescence spectrum $\Lambda(\omega)$, for $\kappa = 100$, $g = 30$, $\gamma = 1$, $\Delta = 0$, $N = 0.5$, $\Omega = 400$, and (a): $\Phi = 0$, $\delta = -\Omega$, (b): $\Phi = 0$, $\delta = 0$, (c): $\Phi = 0$, $\delta = \Omega$, (d): $\Phi = \pi$, $\delta = -\Omega$, (e): $\Phi = \pi$, $\delta = 0$, (f): $\Phi = \pi$, $\delta = \Omega$.

$$\chi_2 = -\frac{i}{2}(1 + \langle\sigma_z\rangle_s - \langle\sigma_y\rangle_s^2 - i\langle\sigma_x\rangle_s\langle\sigma_y\rangle_s),$$

$$\chi_3 = -\frac{1}{2}(1 + \langle\sigma_z\rangle_s)(\langle\sigma_x\rangle_s - i\langle\sigma_y\rangle_s), \tag{23}$$

where $\langle\sigma_i\rangle_s$ ($i = x$, y, z) is the steady-state solutions of Eq. (18).

Figure 3 presents the spectra for $\Omega = 400$, $\Delta = 0$, $N = 0.5$. In the first three frames, Figs. 3a-3c, $\Phi = 0$, and $\delta = -\Omega$, 0, Ω, respectively, while $\Phi = \pi$ in the other frames. As in the absence of the squeezed vacuum [4, 5], the spectral linewidths and heights are dependent on the cavity frequency. When the cavity is tuned to resonance with the laser field, the fluorescence spectrum is symmetric, whilst it is asymmetric when the cavity frequency is tuned to one of the Rabi sidebands. If the cavity frequency is tuned to the lower-frequency sideband, $\delta = -\Omega$, the higher-frequency sideband of the fluorescence spectrum is enhanced, whereas the other peaks are suppressed. The opposite occurs if the cavity frequency tuned to the higher-frequency sideband, $\delta = \Omega$. See, for example Figs. 3a and 3c. These figures also show that all peaks are broadened,
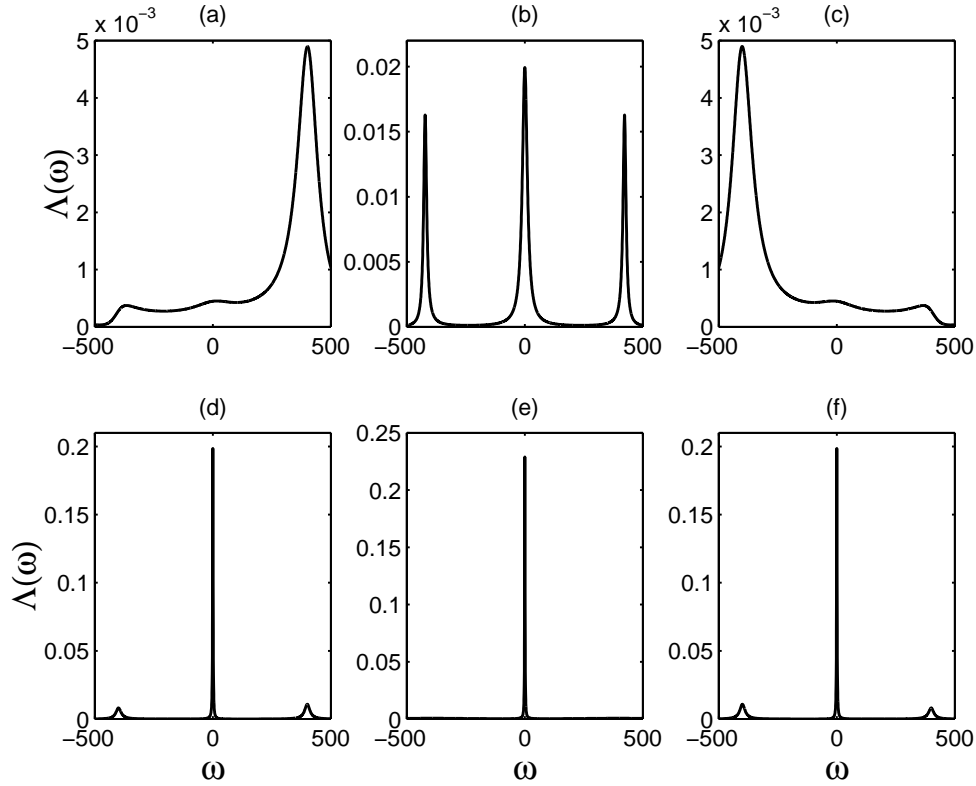
Fig. 4. Same as Fig. 3, but with $N = 5$.

relative to the ones for $\delta = 0$, when the cavity frequency is tuned to one of the Rabi sidebands, but the sideband may be narrower than the central peak. The differences from the standard vacuum case [4, 5] are that the spectrum is phase-sensitive. On comparing Figs. 3d-3f with Figs. 3a-3c, one sees that all spectral lines for the squeezing phase $\Phi = \pi$ are narrower than the corresponding spectral lines for $\Phi = 0$, except for the sidebands in the frame 3e, where the cavity is resonant with the laser field. On the other hand, Figs. 3d-3f also demonstrate that, when $\Phi = \pi$, the linewidth of the sidebands of the fluorescence spectrum for the cavity detuning $\delta = \pm\Omega$ is significantly narrower than that for $\delta = 0$.

We plot the fluorescence spectrum for a large squeezed photon number, $N = 5$, in Fig. 4. In addition to the spectral features shown in Fig. 3 for $N = 0.5$, one may see from Fig. 4b that if the cavity is resonant with the driving laser $\delta = 0$, the sidebands may be made narrower than the central component by increasing the squeezed photon number. On the other hand, for large photon numbers, the sidebands for $\Phi = \pi$ are negligibly small compared to the central peak. The spectrum is almost symmetric when the cavity is detuned from the laser frequency, *e.g.*, in Figs. 4d and 4f.

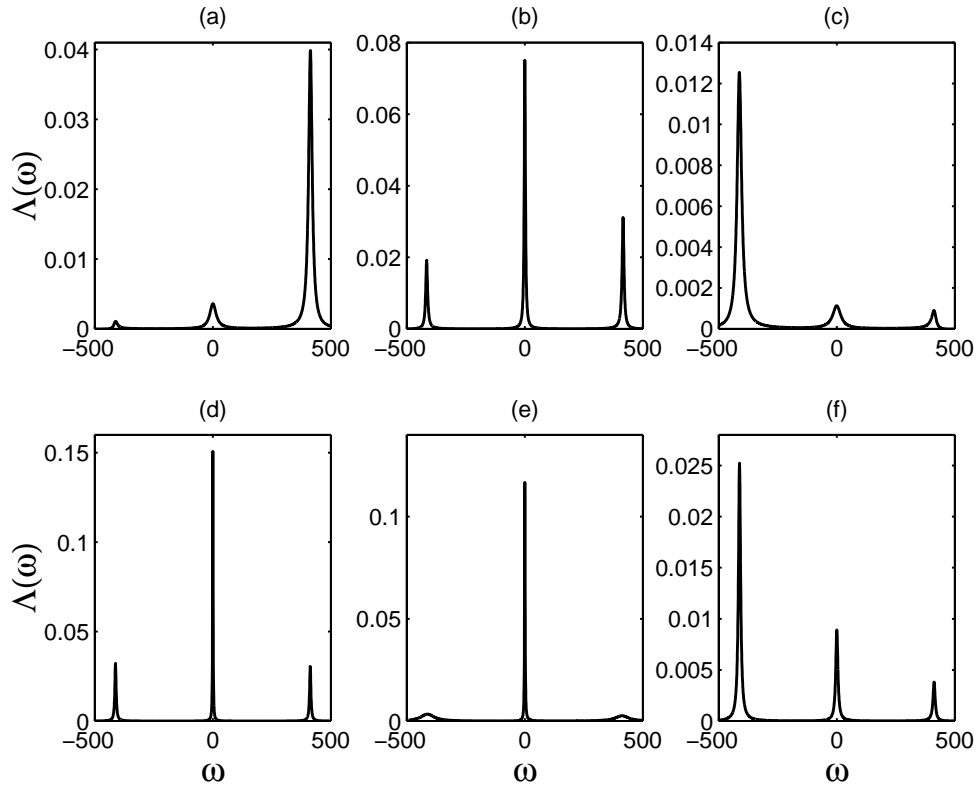Figure 5 displays the spectra when the driving laser is detuned from the atomic

Fig. 5. Same as Fig. 3, but with $\Delta = 100$.

transition frequency, $\Delta = 100$. As for the case $\Delta = 0$, the spectral lines may be narrowed as the squeezing phase Φ varies from 0 to π, and one of the sidebands may be enhanced and the others suppressed if the cavity is detuned from the laser by the Rabi frequency. However, the spectrum for $\Phi = 0$ is, in general, asymmetric even in the case of $\delta = 0$, as we see in Fig. 5b, and the amounts of enhancement and suppression of the spectral lines are also different when the cavity detuning is set to $\delta = \pm\bar{\Omega}$. On the other hand, Figs. 5d and 5e show that for the squeezing phase $\Phi = \pi$, the spectra are almost symmetric when the cavity frequency is tuned to the central and sidebands of the Mollow triplet.

We can gain a physical insight into the narrowing and asymmetries of the cavity-modified Mollow spectrum by employing the semiclassical dressed states $|\pm\rangle$, which are defined via $H_A|\pm\rangle = \pm(\bar{\Omega}/2)|\pm\rangle$. It is well known that the central spectral line results from the atomic downward transitions between the same dressed states of two adjacent dressed-state doublets. The lower-frequency sideband, however, is due to the downward transitions from the substate $|-\rangle$ of one dressed-state doublet to the substate $|+\rangle$ of the next dressed-state doublet, whereas the higher-frequency sideband originates from the downward transitions $|+\rangle \rightarrow |-\rangle$ between two near-lying dressed-state doublets. There-

fore, the central peak is proportional to the product of the two dressed populations, whilst the heights of the lower- and higher-frequency sidebands are associated with the populations of the dressed states $|-\rangle$ and $|+\rangle$, respectively. The linewidths of the centre and sidebands are then determined by the decay rates of the dressed population and coherence, respectively.

We here take $\Delta = 0$ as an example. Under the secular approximation $(\Omega \gg \kappa)$, the populations in the dressed states $|\pm\rangle$ are respectively $\mathcal{P}_{\pm} = (\gamma_x \pm \Omega_1)/2\gamma_x$, and the decay rates of the dressed population and coherence are $\Gamma_{pop} = \gamma_x$ and $\Gamma_{coh} = \frac{1}{2}(\gamma_y + \gamma_z)$, respectively.

When the cavity is resonant with the laser field and atomic transition, *i.e.* $\delta = 0$, then $\Omega_1 = 0$. The spectrum is therefore symmetric, because $\mathcal{P}_+ = \mathcal{P}_- = 1/2$. The linewidths of the central peak and the sidebands are respectively determined by

$$\Gamma_{pop} \simeq \gamma + \gamma_c \left(\frac{\kappa}{\Omega}\right)^2 (2N + 1 + 2M\cos\Phi),$$

$$\Gamma_{coh} \simeq \frac{3\gamma}{2} + \frac{\gamma_c}{2}\left(\frac{\kappa}{\Omega}\right)^2 (2N + 1 + 2M\cos\Phi) + \gamma_c(2N + 1 - 2M\cos\Phi). \quad (24)$$

One sees that the central peak may be narrowed while the sidebands are broadened, as the phase varies from 0 to π. See, for example, the frames (b) and (e) of Figs. 4 and 5. On the other hand, for a squeezed vacuum with a large photon number $(N \gg 1)$ and the relative phase $\Phi = 0$, (24) reduces to

$$\Gamma_{pop} \simeq \gamma + 2\gamma_c \left(\frac{\kappa}{\Omega}\right)^2 (2N + 1),$$

$$\Gamma_{coh} \simeq \frac{3\gamma}{2} + \gamma_c \left(\frac{\kappa}{\Omega}\right)^2 (2N + 1). \quad (25)$$

Therefore, the sidebands can be narrower than the central one, because $\gamma_c \gg \gamma$. For example, in Fig. 4b, $\Gamma_{pop} \sim 13.3$ whilst $\Gamma_{coh} \sim 8$.

When the cavity frequency is tuned to one of the Rabi sidebands, *e.g.* $\delta = -\Omega$, one obtains

$$\Gamma_{pop} \simeq \gamma + \frac{\gamma_c}{2}\left[\left(\frac{\kappa}{2\Omega}\right)^2 + 1\right](2N + 1 + 2M\cos\Phi),$$

$$\Gamma_{coh} \simeq \frac{3\gamma}{2} + \frac{\gamma_c}{4}\left(\frac{\kappa}{2\Omega}\right)^2 (34N + 17 - 30M\cos\Phi) + \frac{\gamma_c}{4}(2N + 1 + 2M\cos\Phi),(26)$$

$$\mathcal{P}_+ \simeq \frac{1}{2\Gamma_{pop}}[\gamma + \gamma_c(2N + 1 + 2M\cos\Phi)],$$

$$\mathcal{P}_- \simeq \frac{1}{2\Gamma_{pop}}\left[\gamma + \gamma_c\left(\frac{\kappa}{2\Omega}\right)^2 (2N + 1 + 2M\cos\Phi)\right]. \quad (27)$$

It is not difficult to see from Eq. (26) that Γ_{pop} and Γ_{coh} decrease as the squeezing phase varies from 0 to π, noting that $(\kappa/\Omega)^2 \ll 1$. For example, in Fig. 3a, $\Gamma_{pop}(\Phi = 0) \sim 17.8$, and $\Gamma_{coh}(\Phi = 0) \sim 10.2$, while $\Gamma_{pop}(\Phi = \pi) \sim 2.2$, and $\Gamma_{coh}(\Phi = \pi) \sim 4.2$ in Fig. 4d.

That is, in the case $\delta = -\Omega$, the sidebands are narrower than the central peak for $\Phi = 0$, whereas for $\Phi = \pi$, they are wider than the central peak. On the other hand, all spectral peaks for $\Phi = \pi$ are narrower than those for $\Phi = 0$. We also find from Eq. (27) that $\mathcal{P}_+ > \mathcal{P}_-$ for all phases, and therefore the higher-frequency sideband peak is higher than the lower-frequency one if the cavity frequency is tuned to the lower-frequency Rabi sideband. Moreover, if $N \gg 1$ and $\Phi = \pi$, then Eq. (27) shows that $\mathcal{P}_+ \sim \mathcal{P}_-$, which means that the spectrum is approximately symmetric—see for example, Figs. 4d and 4f.
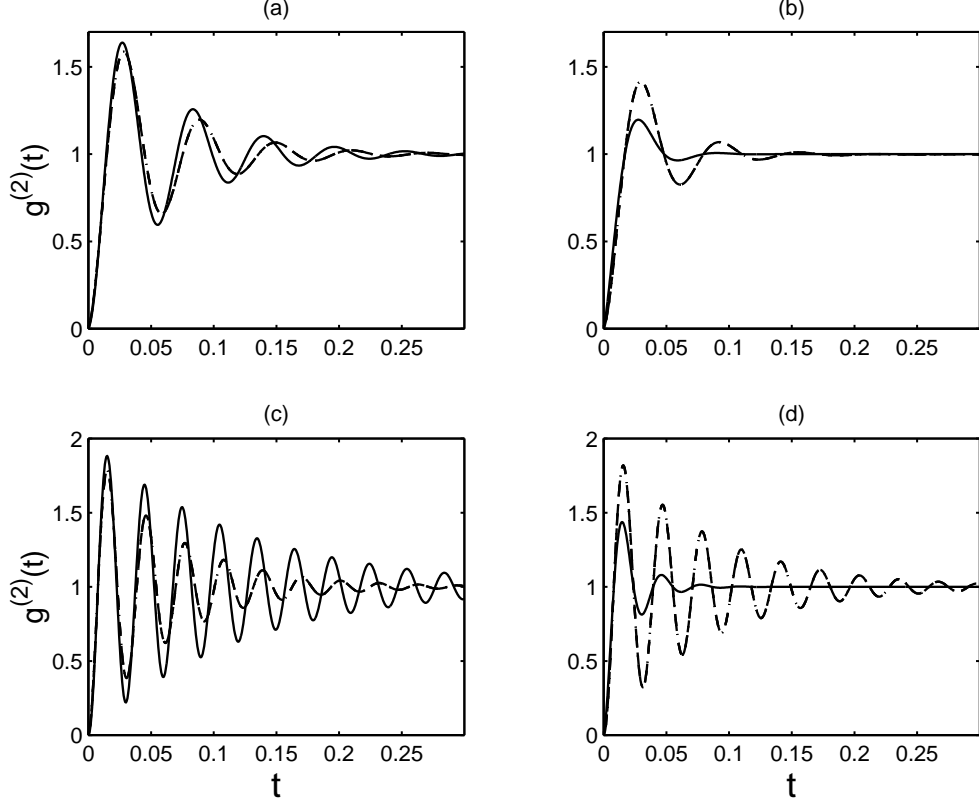

Fig. 6. The second-order intensity correlation $g^{(2)}(t)$, for $\kappa = 100$, $g = 30$, $\gamma = 1$, $\Delta = 0$, $N = 1$, and (a): $\Omega = 100$, $\Phi = 0$, (b): $\Omega = 100$, $\Phi = \pi$, (c): $\Omega = 200$, $\Phi = 0$, (d): $\Omega = 200$, $\Phi = \pi$. The solid curves are for $\delta = 0$, while the dot-dashed curves for $\delta = \pm\Omega$.

3.3. The intensity-intensity correlation

The intensity-intensity correlation function $g^{(2)}(t)$ of the fluorescence field is defined as

$$g^{(2)}(t) = \frac{\langle \sigma_+(0)\sigma_+(t)\sigma_-(t)\sigma_-(0)\rangle_s}{\langle \sigma_+(0)\sigma_-(0)\rangle_s^2}. \tag{28}$$

It is related to the intensity fluctuations of the fluorescence field, and contains information about the probability of detecting a fluorescent photon at time t given that one was detected at time 0.
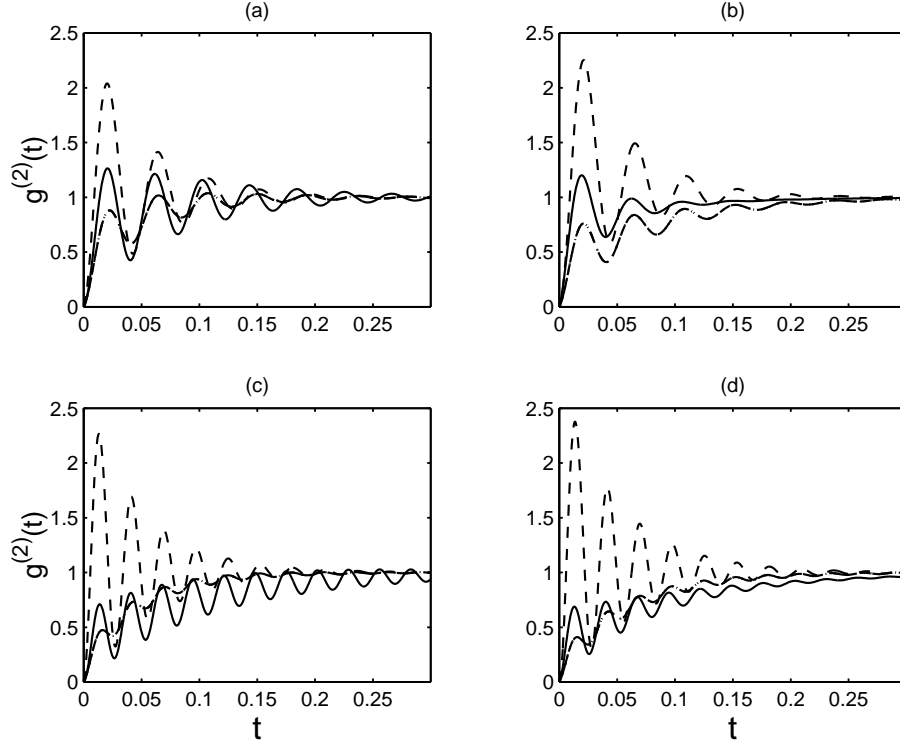

Fig. 7. Same as Fig. 6, but with the parameters: $\kappa = 100$, $g = 30$, $\gamma = 1$, $\Omega = 100$, $N = 1$, and (a): $\Delta = 100, \Phi = 0$, (b): $\Delta = 100$, $\Phi = \pi$, (c): $\Delta = 200, \Phi = 0$, (d): $\Delta = 200$, $\Phi = \pi$. The solid curves are for $\delta = 0$, while the dashed and dot-dashed curves are for $\delta = \bar{\Omega}$ and $-\bar{\Omega}$, respectively.

Figures 6–8 are numerical results of the intensity-intensity correlation function $g^{(2)}(t)$ for various parameters. In Fig. 6 we take $\Delta = 0$, $N = 1$, and (a): $\Omega = 100$, $\Phi = 0$, (b): $\Omega = 100$, $\Phi = \pi$, (c): $\Omega = 200$, $\Phi = 0$ and (d): $\Omega = 200$, $\Phi = \pi$, respectively. In this situation, the functions $g^{(2)}(t)$ for the cavity frequency tuned to either of the Rabi sidebands are identical, and are indicated by the dot-dashed curves. The solid curves, however, are the intensity-intensity correlation $g^{(2)}(t)$ for the cavity tuned to resonance with the laser field. Interestingly, the value of $g^{(2)}(t)$ varies dramatically with the cavity frequency, as well as the squeezing phase. For $\Phi = 0$ the amplitudes of the oscillations of the second-order correlation function $g^{(2)}(t)$ with the cavity detuning $\delta = 0$ are larger than those with $\delta = \pm\Omega$. For $\Phi = \pi$ however, the opposite results are obtained.

We plot the function $g^{(2)}(t)$ for different cavity-laser and atom-laser detunings in Fig. 7, which results in different values of $g^{(2)}(t)$ for $\delta = \pm\bar{\Omega}$. The oscillations of $g^{(2)}(t)$

for $\delta = \bar{\Omega}$ are stronger than those for the other detunings, $\delta = 0$ and $-\bar{\Omega}$. The latter exhibits the photon antibunching effect, $i.e.$, $g^{(2)}(t) < 1$. Although the photon anti-bunching of the fluorescence field was predicted and observed in free space [24], it occurs for weak Rabi frequencies ($\Omega \leq \gamma$). The photon antibunching predicted here, however, occurs at strong Rabi frequency regimes ($\Omega \gg \gamma$), and depends upon the cavity resonant frequency and squeezing phase.
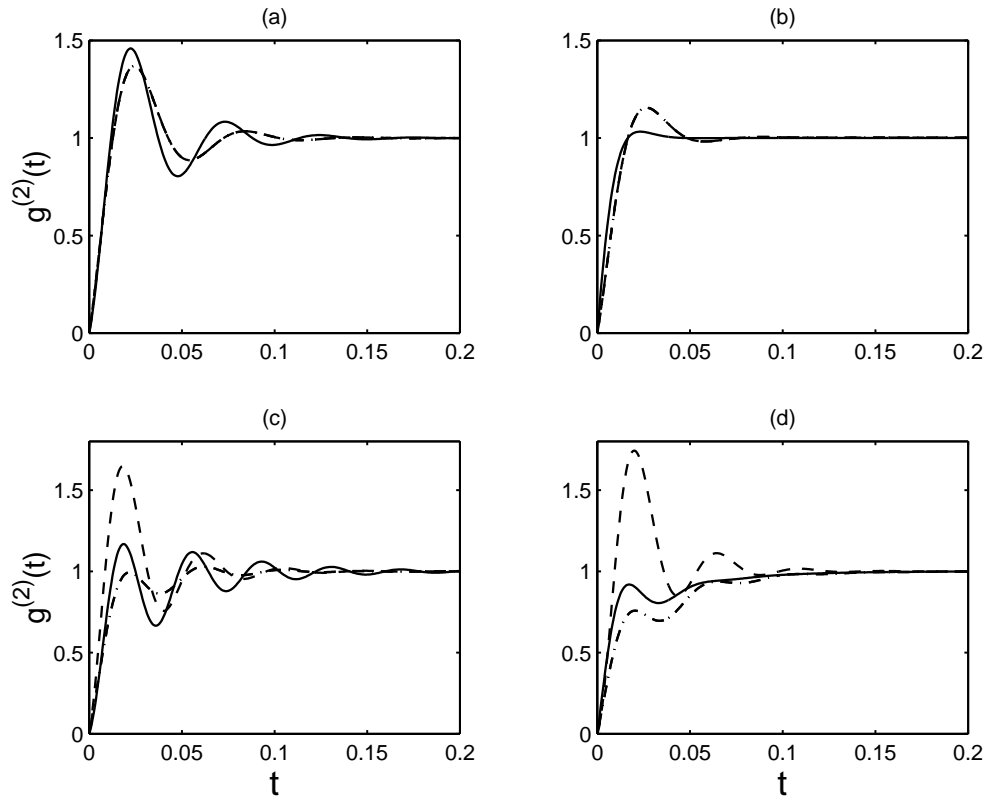

Fig. 8. Same as Fig. 6, but with the parameters: $\kappa = 100$, $g = 30$, $\gamma = 1$, $\Omega = 100$, $N = 3$, and (a): $\Delta = 0, \Phi = 0$, (b): $\Delta = 0$, $\Phi = \pi$, (c): $\Delta = 100, \Phi = 0$, (d): $\Delta = 100$, $\Phi = \pi$. All solid curves in the frames (a)–(d) are for $\delta = 0$. The dot-dashed curves are for $\delta = \pm\bar{\Omega}$ in the frames (a) and (b). Whereas, the dashed and dot-dashed curves in the frames (c) and (d) are for $\delta = \bar{\Omega}$ and $-\bar{\Omega}$, respectively.

Figure 8 is the correlation function for a large squeezing photon number, $N = 3$. The amplitudes of the oscillations decrease very quickly, because of the increase of the decay rates with large squeezed photon number.

As we know, the intensity-intensity correlation function $g^{(2)}(t)$ may be simply interpreted as the probability for finding an initially unexcited atom in its upper state [24]. The probability can be obtained by solving the Bloch equation (18). Qualitatively, we conclude that the probability oscillates at the generalized Rabi frequency

$\bar{\Omega} = \sqrt{\Omega^2 + \Delta^2}$, with the amplitudes undergoing an exponential decay at rates associated with γ_x, γ_y and γ_z. Due to the dependence of these decay rates γ_x, γ_y, γ_z on the cavity resonant frequency, the driving laser frequency and intensity, and the squeezing photon number and phase, the probability, and therefore the intensity-intensity correlation $g^{(2)}(t)$, varies with these different parameters.

4. Summary

We have studied the modification of the resonance fluorescence from a strongly driven two-level atom located inside a frequency-tunable cavity which is damped by a broadband squeezed vacuum. In the bad cavity limit, we derived an effective master equation for the reduced density matrix operator for this system, which exhibits resonance properties when the cavity frequency is tuned to the centre and sidebands of the standard Mollow triplet. We find that the intensity, resonance fluorescence spectrum and photon-photon correlation function are all strongly dependent upon the cavity resonance frequency and squeezing phase. The fluorescence intensity of the atom emitted from the side (mirror) of the cavity can be enhanced or suppressed by appropriately tuning the cavity frequency to the central peak or Rabi sidebands of the standard Mollow triplet, and varying the squeezing phase. The spectral lines can be also enhanced or suppressed in a prescribed manner by changing these parameters. In general, the central peak and one sideband of the fluorescence spectrum are suppressed when the cavity is tuned to resonance, whilst the other sideband is enhanced. For certain parameters, the sidebands may be narrower than the central peak. All spectral lines for $\Phi = 0$ are broader than the ones for $\Phi = \pi$. The fluorescence field can also exhibit the photon antibunching effect for some cavity and laser frequencies and squeezed phase in the strong Rabi frequency regime.

References

[1] For recent reviews, see, for example, *Cavity Quantum Electrodynamics*, ed. by P.R. Berman (Academic Press, Inc., London, 1994)

[2] E.M. Purcell: *Phys. Rev.* **69** (1946) 681; D. Kleppner: *Phys. Rev. Lett.* **47** (1981) 233

[3] P. Goy, J.M. Raimond, M. Gross, S. Haroche: *Phys. Rev. Lett.* **50** (1983) 1903; D.P. O'Brien, P. Meystre, H. Walther: *Adv. At. Mol. Phys.* **21** (1985) 1; R.G. Hulet, E.S. Hilfer, D. Kleppner: *Phys. Rev. Lett.* **55** (1985) 2137; D.J. Heinzen, M. S. Feld: *Phys. Rev. Lett.* **59** (1987) 2623; W. Jhe, A. Anderson, E.A. Hinds, D. Meschede, L. Moi, S. Haroche: *Phys. Rev. Lett.* **58** (1987) 666; D.J. Heinzen, J.J. Childs, J.E. Thomas, M.S. Feld: *Phys. Rev. Lett.* **58** (1987) 1320; F. De Martini, G.R. Jacobovitz: *Phys. Rev. Lett.* **60** (1988) 1711

[4] M. Lewenstein, T.W. Mossberg, R.J. Glauber: *Phys. Rev. Lett.* **59** (1987) 775; M. Lewenstein, T.W. Mossberg: *Phys. Rev. A* **37** (1988) 2048

[5] P. Zhou, S. Swain: *Phys. Rev. A* **57**, No.6 (1998) in press

[6] T. Quang, H. Freedhoff: *Phys. Rev. A* **47** (1993) 2285; H. Freedhoff, T. Quang: *Phys. Rev. Lett.* **72** (1994) 474; H. Freedhoff, T. Quang: *J. Opt. Soc. Am. B* **10** (1993) 1337; **12** (1995) 9

[7] J.I. Cirac, H. Ritsch, P. Zoller: *Phys. Rev. A* **44**(1991) 4541; M. Loffler, G.M. Meyer, H. Walther: *Phys. Rev. A* **55**(1997) 3923

[8] W. Lange, H. Walther: *Phys. Rev. A* **48** (1993) 4551; G. S. Agarwal, W. Lange, H. Walther: *Phys. Rev. A* **48** (1993) 4555

[9] Y. Zhu, A. Lezama, T. W. Mossberg: *Phys. Rev. Lett.* **61** (1988) 1946; A. Lezama, Y. Zhu, S. Morin, T. W. Mossberg: *Phys. Rev. A* **39** (1989) R2754

[10] C.W. Gardiner: *Phys. Rev. Lett.* 56 (1986) 1917; A.S. Parkins, C. W. Gardiner: *Phys. Rev. A* **40** (1989) 3796

[11] H. J. Carmichael, A. S. Lane, D. F. Walls: *Phys. Rev. Lett.* **58** (1987) 2539; *J. Mod. Opt.* **34** (1987) 821

[12] J. M. Courty, S. Reynaud: *Europhys. Lett.* **10** (1989) 237; P.R. Rice, L. M. Pedrotti: *J. Opt. Soc. Am. B* **9** (1992) 2008; W.S. Smyth, S. Swain: *Phys. Rev. A* **53** (1996) 2846; P. Zhou, S. Swain: *Opt. Commun.* **131** (1996) 153; P.R. Rice, C.A. Baird: *Phys. Rev. A* **53** (1996) 3633; P. Zhou, Z. Ficek, S. Swain: *Opt. Commun.* **148** (1998) 159

[13] J.I. Cirac: *Phys. Rev. A* **46** (1992) 4354

[14] C.M. Savage: *Quantum Opt.* **2** (1990) 89; A.S. Parkins, P. Zoller, H.J. Carmichael: *Phys. Rev. A* **48** (1993) 758

[15] C. Cabrillo, S. Swain: *Phys. Rev. Lett.* **77** (1996) 478

[16] N.Ph. Georgiades, E.S. Polzik, K. Edamatsu, H.J. Kimble, A.S. Parkins: *Phys. Rev. Lett.* **75** (1995) 3426

[17] P. Zhou, S. Swain: *Phys. Rev. A* **54** (1996) 2455; *Opt. Commun.* **134** (1997) 127

[18] S. Smart, S. Swain: *Phys. Rev. A* **48** (1993) R50; S. Swain: *Phys. Rev. Lett.* **73** (1994) 1493; S. Swain, P. Zhou: *Phys. Rev. A* **52** (1995) 4845; P. Zhou, Z. Ficek, S. Swain: *J. Opt. Soc. Am. B* **13** (1996) 768

[19] Z. Ficek, W.S. Smyth, S. Swain: *Opt. Commun.* **110** (1994) 555; *Phys. Rev. A* **52** (1995) 4126

[20] S.M. Barnett, P.L. Knight: *Phys. Rev. A* **33** (1986) 2444

[21] B.R. Mollow: *Phys. Rev.* **188** (1969) 1969; F.Y. Wu, R.E. Grove, S. Ezekiel: *Phys. Rev. Lett.* **35** (1977) 1426

[22] C. Cohen-Tannoudji, S. Reynaud: in *Multiphoton Processes*, eds. by J.H. Eberly and P. Lambropoulos (Wiley, New York, 1978); *J. Phys. B* **10** (1977) 345

[23] C.M. Savage: *Phys. Rev. Lett.* **60** (1988) 1828; M. Lindberg, C.M. Savage: *Phys. Rev. A,* **38** (1988) 5182

[24] D.F. Walls, G.J. Milburn: *Quantum Optics* (Spring-Verlag, Berlin, 1994) Chap. 11; and references therein